Biomass Conv. Bioref. (2018) 8:19–31
DOI 10.1007/s13399-016-0225-7

ORIGINAL ARTICLE

Thermodynamic equilibrium analysis of entrained flow gasification of spent pulping liquors

Erik Furusjö[1] · **Yawer Jafri**[1]

Received: 31 August 2016 / Revised: 10 October 2016 / Accepted: 26 October 2016 / Published online: 11 November 2016

Abstract The main goal of this work is to investigate if thermodynamic equilibrium calculations can be useful for understanding and predicting process performance and product composition for entrained flow gasification of spent pulping liquors, such as black liquor. Model sensitivity to input data is studied and model results are compared to published pilot plant data. The high temperature and the catalytic activity of feedstock alkali make thermodynamic equilibrium a better predictor of product composition than for many other types of biomass and gasification technologies. Thermodynamic equilibrium calculations can predict the flows of the main syngas and slag products with high accuracy as shown by comparison with experimental data with small measurement errors. The main process deviations from equilibrium are methane formation and sulfur distribution between gas and slag. In order to study real process deviations from equilibrium, it is very important to use consistent experimental data. Relatively small errors in the model input, primarily related to fuel composition, can lead to grossly erroneous conclusions. The model sensitivity to fuel composition also shows that the gasification process is sensitive to naturally occurring feedstock variations. Simulations of a commercial-scale gasification process show that cold gas efficiency on sulfur-free basis can reach over 80 % and that greatly improved efficiency can be obtained by reducing ballast present in the form of water or inorganics.

Keywords Biomass gasification · Thermodynamic equilibrium · Black liquor · Sulfite thick liquor · Pilot plant

Abbreviations

BL	Black liquor
BLG	Black liquor gasification
CGE	Cold gas efficiency
EF	Entrained flow
EFG	Entrained flow gasification
ESP	Electrostatic precipitator
GL	Green liquor
HHV	Higher heating value
LHV	Lower heating value
MC	Monte Carlo
OP	Operating point
RB	Recovery boiler
STL	Sulfite thick liquor
TEC	Thermodynamic equilibrium calculation
TIC	Total inorganic carbon

1 Introduction

Biomass gasification is a promising technology for production of second-generation biofuels and green chemicals. Many gasification technologies produce syngas with high concentrations of tars, which leads to extensive gas cleaning requirements. Entrained flow (EF) gasifiers, using higher temperatures and short residence times, often generate a relatively clean gas and can use no or much simpler gas cleaning. A potential drawback of EF gasification (EFG) is the

Electronic supplementary material The online version of this article (doi:10.1007/s13399-016-0225-7) contains supplementary material, which is available to authorized users.

✉ Erik Furusjö
erik.furusjo@ltu.se

[1] Division of Energy Sciences, Luleå University of Technology, SE-971 87 Luleå, Sweden

requirement to feed solid fuels in a pulverized form, while liquid feedstocks can be atomized.

An EFG technology that has come a long way towards commercialization, through demonstration of an integrated biomass-to-biofuel process, is black liquor gasification (BLG) [1]. Black liquor (BL) is a by-product of Kraft pulping that contains dissolved lignin and hemicellulose fragments together with spent inorganic pulping chemicals. It is normally combusted in a recovery boiler (RB) that recovers inorganic pulping chemicals and generates steam. It has been shown that higher overall efficiency and better profitability can be obtained by gasifying BL and generating the process steam from other fuels [2–5].

The EF BLG process has been demonstrated and investigated in pilot scale using Kraft BL [1, 6–10] and sulfite thick liquor (STL) [11, 12]. The latter is the spent pulping liquor from sodium-based sulfite delignification. EF gasification of BL and STL is carried out under slagging conditions at 1000–1100 °C. The inorganic smelt (slag) leaving the gasifier is dissolved in water to form a solution called green liquor (GL), which is used to recover the inorganic pulping chemicals.

It has generally been established that thermodynamic equilibrium calculations (TECs) are useful for understanding the behavior of biomass gasification under varying process conditions for a range of fuel compositions [13–15]. In practice, deviations from equilibrium are common and relate for example to char conversion, tar formation, methane formation, and the water gas shift reaction, especially for low-temperature processes [16–18]. Cold gas efficiency (CGE), which controls the potential biofuels yield, is of general interest to predict and understand in biomass gasification while the sulfur distribution between gas and slag phases, which is very important for the recovery of the pulping chemicals (below referred to as the sulfur split), is more specific for BLG.

Ash is typically either disregarded or considered inert when developing thermodynamic equilibrium models for non-slagging fixed bed and fluidized bed gasifiers [18–20]. For entrained flow gasification of solid biomass, however, slag properties are important and TECs have proven useful for understanding and predicting such properties [21, 22]. Treating ash as inert in gasification of sodium-rich fuels such as BL or STL would give totally misleading results since approximately 20 % of the carbon leaves the reactor in the inorganic smelt [6].

Previously, Berglin [23] used a simplified thermodynamic equilibrium model only for the gas phase, aiming to study the performance of air-blown BLG for electricity production. Other thermodynamic equilibrium studies of BLG included slag species in the models [7, 10, 24–26]. However, the few studies that compared their results to experimental data only focused on equilibrium gas composition and did not validate the composition of the inorganic phase [7, 10]. The properties of the inorganic smelt are very important in gasification of BL and STL since it is used to form the aqueous GL that enables to reuse of the pulping chemicals [6, 12]. In addition, the inorganic phase influences the mass and energy balances for the gasifier substantially.

In summary, there are no studies applying TECs to STL gasification and only two studies comparing TECs for BL gasification to experimental syngas data, neither of which validated prediction of the inorganic phase against experimental results. Hence, better validation is needed under a range of process conditions to reliably and consistently use TECs for studying spent pulping liquor gasification. The main goals of this work are to assess if TECs can be useful for predicting process performance and product composition for EFG of spent pulping liquors as well as quantifying and understanding deviations between model and experimental data.

The techno-economic studies of BLG-based biorefineries use fixed BL properties and process design relevant for the cases studied [5, 27]. However, many parameters with substantial impact on the process performance can be influenced through the process design. A second goal of this work is to use a validated thermodynamic equilibrium model to quantify the impact of important design parameters on the gasification performance and syngas properties for a commercial-scale gasification process.

In principle, any observed differences between TEC results and experimental data can be due to real deviations from equilibrium in the process, erroneous experimental data, and erroneous inputs to the equilibrium model or any combination of these. In order to understand the influence of each of potential cause of deviation, we start by investigating the sensitivity of the TEC to input data followed by an analysis of the deviations for the pilot plant cases studied. The last part of this study uses TEC to predict the behavior of a commercial-scale gasification process.

2 Materials and methods

2.1 Pilot plant data

This work uses previously published data from three studies [6, 10, 12] of the BLG pilot plant in Piteå, Sweden, to obtain relevant operating conditions for TECs and to compare predictions to experimental results. The reader is referred to those studies as well as other experimental studies [8, 9] for a description of the pilot plant and the process.

The experiments described and analyzed by Jafri et al. [6] used BL from the Smurfit Kappa Kraftliner mill (Piteå, Sweden) as feedstock. The data includes five operating points (OPs) at 2.6–3.1 MW_{th} load and 24–29 bar. The data in Wiinikka et al. [10] is based on experiments using the same feedstock source. Six OPs with a load around 3 MW_{th} and

varying pressure (25–29 bar) and temperature were investigated. The experiments presented by Furusjö et al. [12] used STL from the Domsjö Fabriker (Örnsköldsvik, Sweden) sodium sulfite-based delignification process, which has significantly different properties from BL as discussed further below.

The Furusjö and Jafri data quantifies both syngas and inorganic GL components and thus allows full mass and energy balances to be made. Wiinikka et al. only presents data for the syngas. Hence, no balances can be made and no comparison between model and experiment are possible for inorganic components in this case.

It is difficult to measure process temperatures accurately [6, 12], but the shielded thermocouples used are still considered to give reasonable temperature values that can be used to observe trends and differences between OPs. In practice, syngas methane concentration is used as a temperature proxy and is set to approximately 1 % for "standard" operation by varying the amount of oxygen added to the gasifier.

The measured reactor temperatures used in this work for the Jafri et al. data set are slightly different (10–20 °C higher) from the values presented in the original paper. This is due to the fact that an average of two thermocouples positioned in the mid-level of the reactor was used, whereas Jafri et al. presented values for one of these. The Wiinikka et al. temperature data is based on a thermocouple in the same position. For the Furusjö et al. data, temperatures from the thermocouple positioned close to the bottom of the reactor were used.

2.2 Thermodynamic equilibrium calculations

TECs were carried out using FactSage (GTT-Technologies, Aachen, Germany) as well as an in-house tool called SIMGAS, which was developed in the Matlab environment (Mathworks, Natick, MA, USA). Both tools use a non-stoichiometric approach since stoichiometric methods are not suitable for complex multicomponent systems. In comparison to FactSage, SIMGAS uses a simpler thermodynamic model, including only ideal mixtures of components for both the gas and the inorganic smelt phases. Included components are listed in Table 1; this selection is based on species for which significant concentrations were found during numerous runs with varying process conditions. The pure component data for gas components and solid carbon are taken from the NIST Chemistry WebBook while data for pure inorganic smelt components are based on Lindberg [28]. In SIMGAS, Gibbs energy minimization is accomplished using an active-set method in order to be able to include both linear and non-linear constraints.

Initially, a comparison between FactSage and SIMGAS results was made in order to assess the influence of the simpler thermodynamic model in SIMGAS. This comparison between the two thermodynamic models is described in Section 2 of the Supplementary Material. The conclusion is that the simpler implementation in SIMGAS is sufficient to describe the process for the purposes of this study. No significant differences were observed for major species. Hence, the remainder of the work described in this paper is based on the SIMGAS model. However, if the aim is to study smelt properties or smelt reactions, the more sophisticated smelt model of FactSage would be required. The primary motivation for using the Matlab-based SIMGAS tool is the ease with which constraints can be implemented in order to be able to model deviations from equilibrium in some cases.

Table 1 Pure components included in the SIMGAS Gibbs energy minimization

Gas	Solid/liquid
H_2(g)	Na_2CO_3(l)
CO(g)	Na_2S(l)
CO_2(g)	NaOH(l)
H_2O(g)	NaCl(l)
CH_4(g)	Na_2SO_4(l)
H_2S(g)	K_2CO_3(l)
COS(g)	K_2S(l)
N_2(g)	KOH(l)
	KCl(l)
	K_2SO_4(l)
	C(s)

In practical application of EF biomass gasification, temperature is controlled by oxygen addition, i.e., the process is autothermal. For simulation of pilot plant OPs, TECs are executed in a mode where the temperature of the products is calculated based on an energy balance over the gasification process. For the simulation of commercial biorefinery gasification operation, a certain gasifier temperature is specified and the required amount of oxygen to reach this temperature is calculated through the gasifier energy balance.

For the gas phase, comparison between model results and experimental data is straightforward. The inorganic smelt is, however, dissolved to form GL. In this work, the experimentally determined concentrations of inorganic components in GL are compared to TEC smelt predictions. The components are sulfur, carbonate, and total inorganic carbon (TIC). TIC is the sum of carbon present as carbonate and hydrogen carbonate. Hydrogen carbonate is not present in the smelt leaving the gasifier but is formed in the quench as discussed below. Sodium and potassium are not compared since according to both model and experimental data, they are found solely in GL.

2.3 Feedstock heat of formation

Solving the gasifier energy balance during TECs requires knowledge of the enthalpies of all streams entering and leaving the process. The enthalpy can be defined with respect to

any reference condition. In this work, the selected reference condition is the elements at standard reference state, which means that the enthalpy describing chemical energy is the heat of formation. For the oxygen, nitrogen, and gasification products, enthalpy estimation is straightforward since the chemical composition is known. However, for the spent pulping liquors, which are highly complex mixtures of organic and inorganic species, it is not possible to use tabulated data for heat of formation. Instead, their enthalpies of formation are calculated from higher heating values (HHV) determined by bomb calorimetry using Hess' law in conjunction with assumptions about the bomb combustion products as described earlier [6]. When this approach is used, it is very important to know exactly which heating value is measured, i.e., what are the final combustion products in the bomb calorimeter? Spent pulping liquors of the type studied in this work are characterized by high sodium and sulfur contents, which are typically 20 and 5 % on a dry-weight basis, respectively.

The bomb product chemistry is investigated in some detail in the Supplementary Material. The main conclusion is that due to the presence of high amounts of inorganics in the fuel, carbon ends up as a mixture of carbon dioxide and sodium carbonate. Sulfur ends up as sodium sulfate or sodium hydrogen sulfate depending on the sodium/sulfur ratio. This is different from assumptions typically used for low ash fuels.

3 Results and discussion

3.1 Model sensitivity to input data

The inputs to a thermodynamic equilibrium model for a gasification process consist of the flow, temperature and composition of the streams entering the gasification reactor, and the reactor heat loss in combination with the thermodynamic data/assumptions. In the present case, there are three streams: spent pulping liquor, oxygen, and nitrogen. The nitrogen flow is very small compared to the other flows and does not have a direct impact on the process (except as thermal ballast).

The pilot plant from which all experimental data used in this work comes is equipped with Coriolis type mass flow meters for both oxygen (Krohne Optimass 1300; KROHNE Messtechnik GmbH, Duisburg, Germany) and feedstock (Yokogawa Rotamass 3 series; Yokogawa Electric Corporation, Tokyo, Japan). According to the instrument specifications, the measurement error is typically around 0.2 %. In our experience, a larger uncertainty can be expected in practice; we have used a 95 % confidence interval of ±1 % in the sensitivity analysis below.

The oxygen and nitrogen compositions are well known since they are of high purity. Feedstock elemental analysis for BL and STL is associated with a relatively large uncertainty as summarized in Table 2 based on uncertainty estimates from the experimental studies. Uncertainty estimates are only available for BL and do not agree fully between the two studies. A pooled relative standard deviation for each element was calculated based on the 95 % confidence limits provided in the earlier work and assuming these to have the same number of degrees of freedom as shown in Table 2 (rightmost column). From the standard deviation presented in Table 2, it is clear that the uncertainty in most elements is relatively large.

Figure 1 shows results from varying selected inputs to the upper and lower 95 % confidence limits (as approximated by ±2 pooled standard deviations) for a selected operating point (Jafri et al. OP 5). It can be concluded that black liquor composition uncertainty contributes significantly to variation in the model outputs, while the contribution from flow measurement uncertainty seems to be less important. As an example, the carbon content uncertainty leads to predicted temperatures in a range of 1077–1286 °C. This range is much larger than the practical operating envelope of the gasifier [6], which should have significant consequences on agreement between model outputs and experiments, as discussed further below. The variation in cold gas efficiency due to carbon analysis uncertainty is approximately ±5 % units, which is a very significant number and corresponds to approximately ±9 % relative uncertainty. When compared with the ±2.6 % relative uncertainty ($2s_{rel}$) for the BL C analysis, it is easy to conclude that input errors are amplified in the model. The influence of BL sodium content uncertainty is even larger than that of carbon while it is slightly smaller for hydrogen. Figure 1 also shows the influence of composition measurement uncertainty on the sulfur split and the hydrogen/carbon monoxide ratio in the syngas, which are important properties for the design of a spent pulping liquor gasification-based biorefinery.

From the above results, it is clear that BL composition is a major contributory factor to the uncertainty in TEC results. It is, however, likely that the influence of individual component uncertainty is not a good measure of the total influence on the TECs. In order to estimate the effect of the combined uncertainty of all BL constituents, a Monte Carlo (MC) simulation was carried out. All BL elements except oxygen were assumed to have independent errors with a normal distribution and a standard deviation according to the pooled relative standard deviation presented in Table 2. Feedstock oxygen content was calculated by difference as it is typically done in BL element analysis. In this study, 8000 cases were simulated using TECs with stochastic input data to generate a distribution of all model results, as shown for temperature in Fig. 2. Only BL composition was accounted for in the MC study, although it would have been feasible to include also other uncertain model inputs simultaneously.

From the MC simulation results presented in Fig. 1, it is clear that the uncertainty from the combined BL constituents is greater than that from individual components or other factors studied. The results presented in Fig. 1 represent 95 %

Table 2 Element composition and heating value, including uncertainties presented in the references, for the experimental data used in this work (s_{abs} and s_{rel} indicate absolute and relative standard deviation, respectively)

		Jafri et al. [6]			Wiinikka et al. [10]			Furusjö et al. [12]	Pooled[c]
		BL	$2s_{abs}$[a]	s_{rel}[b]	BL	$2s_{abs}$[a]	s_{rel}[b]	STL	s_{rel}
C	m/m	27.5 %	0.55 %	1.0 %	31.2 %	0.93 %	1.5 %	42.5 %	1.3 %
H	m/m	3.75 %	0.23 %	3.1 %	3.30 %	0.12 %	1.8 %	4.15 %	2.5 %
N	m/m	0.07 %	0.02 %	14.3 %	0.09 %	0.01 %	5.6 %	0.88 %	10.8 %
Cl	m/m	0.16 %	0.02 %	6.3 %				0.01 %	6.3 %
Na	m/m	19.9 %	3.97 %	10.0 %	21.2 %	0.92 %	2.2 %	8.5 %	7.2 %
K	m/m	3.12 %	0.62 %	9.9 %	2.85 %	0.31 %	5.4 %	0.15 %	8.0 %
S	m/m	6.20 %	1.24 %	10.0 %	6.10 %	0.71 %	5.8 %	9.40 %	8.2 %
O	m/m	39.35 %			35.26 %			34.42 %	
HHV	MJ/kg	12.13	0.20	0.8 %	12.75	0.30	1.2 %	18.36	1.0 %
DS[d]	m/m	71.7 %			73.1 %			58–63%[e]	

[a] Uncertainty specified in the references is interpreted as having a coverage factor of two, i.e., representing an approximate 95 % confidence interval

[b] Relative standard deviation calculated based on two previous columns

[c] Pooled relative standard deviation based on uncertainty data from Jafri et al. and Wiinikka et al.

[d] Dry solids content on mass basis

[e] Varying dry solids content for the OPs, see original work [12]

confidence intervals obtained from the 2.5 and 97.5 % percentiles of the MC output distributions, as exemplified in Fig. 2. The 95 % intervals for the reactor temperature and H_2/CO are 960–1409 °C and 0.81–1.65, respectively. It can also be noted

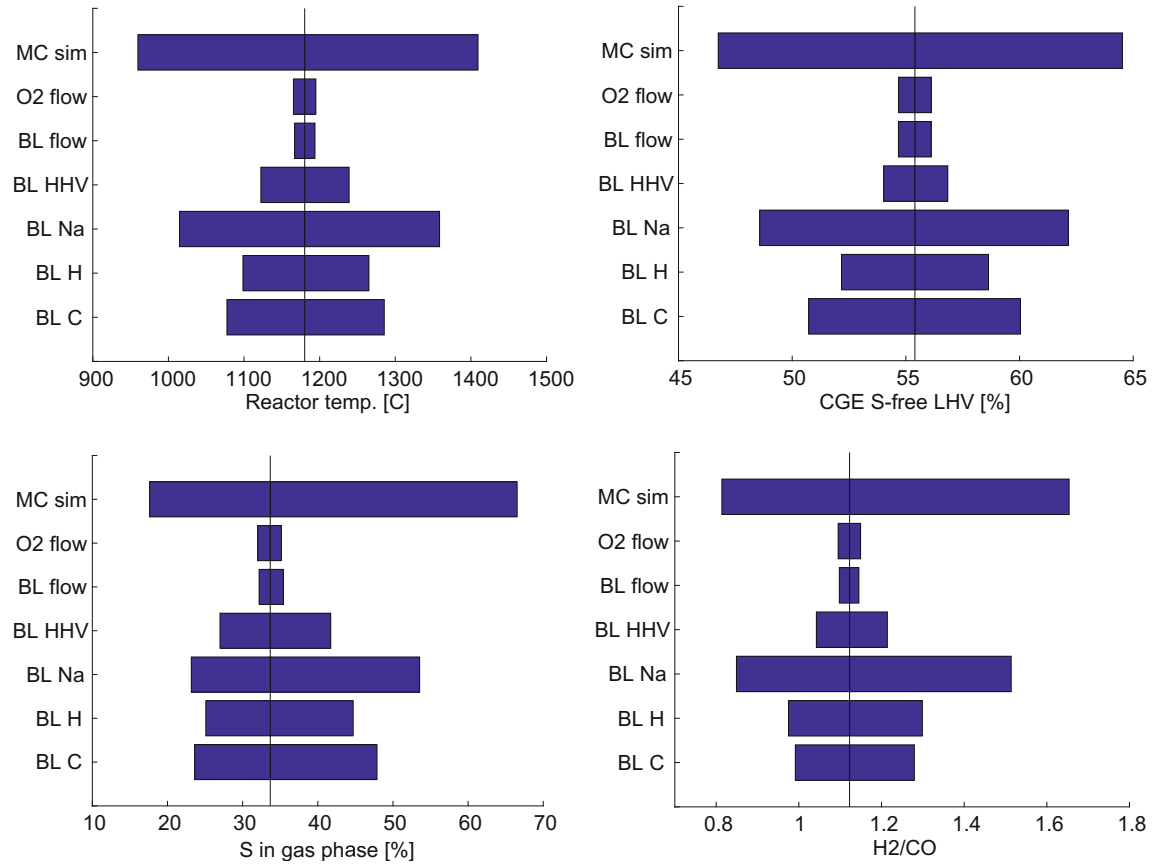

Fig. 1 Influence on selected TEC results from uncertainty in model inputs. The *vertical line* is the model prediction for the base case. Model inputs were varied one at a time according to estimated 95 % confidence limits with the exception of the bars labeled "MC sim" in which all BL constituents were varied simultaneously (see text)

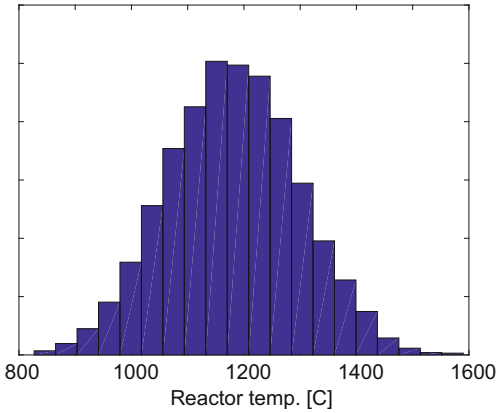

Fig. 2 Distribution for reactor temperature resulting from the MC simulations based on uncertainty in BL composition

that the uncertainty in fuel composition creates an uncertainty in oxygen content and stoichiometric oxygen demand. The Monte Carlo simulation gives a 95 % confidence interval for stoichiometric oxygen demand of 0.75–0.86 kg O/kg BL, which clearly indicates that lambda is not always a well-determined parameter for experimental data. The BL oxygen content distribution had a standard deviation of 1.6 % (absolute) or 4.0 % (relative).

The investigations described in this section show that input parameter uncertainty influences the TEC results to a great extent. This can be problematic when using TECs to predict gasification process performance as shown further below.

3.2 Sensitivity to feedstock heat of formation estimation

An important thermodynamic assumption made is related to the calculation of feedstock heat of formation estimation. For low ash fuels, the assumptions about bomb calorimeter combustion products are not so important, but for high ash and high sulfur fuels, such as the spent pulping liquors studied in this work, the issue is more important and complex. The approach described in Section 2.3 and in more detail in the Supplementary material is typically used for BL, but we also evaluated a simplified approach based on the assumption that alkali metals form oxides, as is typically done in ash analysis of biomass.

Assuming that sodium and potassium form oxides (as opposed to carbonates and sulfates), all sulfur forms sulfur dioxide (as opposed to sulfate) and all carbon forms carbon dioxide (as opposed to a mix of carbonate and carbonate dioxide); the calculated BL heat of formation values are 1.6–2.3 MJ/kg solids higher for the liquor compositions studied in this work, which corresponds to approximately 10–20 % of HHV. The resulting error completely changes the results of the TECs. This highlights how critical it is to make correct assumptions about the bomb calorimeter combustion products. According to Table 2, the relative standard deviation for HHV is 1 %. Hence, the assumption about combustion products has a much larger impact on TECs than the actual HHV measurement error.

3.3 Agreement between pilot plant data and equilibrium calculations

3.3.1 Non-constrained equilibrium calculations

Operating data in the form of fuel flow rate, fuel composition, oxygen flow rate, nitrogen flow rate, and process pressure were used in TECs representing each OP in the data sources, with the exception of OP2 of Furusjö et al., which was excluded due to very poor experimental balance closures (−18 % for total mass, −30 % for carbon) [12]. Comparisons between experimental data and model predictions are shown in Figs. 3, 4, and 5.

The difference between measured and calculated temperatures, shown in Fig. 3, is up to 185 °C. This is very high compared to the span in the experimental data but not greater than the deviations shown possible to result from uncertainty in BL composition (cf. Fig. 1). It is very clear that while the correlation between model and experimental temperature within each data set is very strong, there are large differences between the data sets. The two BL fuel data sets that use BL from the same mill have deviations of opposite sign. This points clearly to that reasons for the temperature deviations are specific to a whole data set but not to the fuel type. Such a factor can be data set wide systematic errors in flow measurements or fuel composition; a single fuel composition is used for all OPs in each data set as discussed above. Considering the simulation results in Fig. 1 and the magnitude of the differences in Fig. 3, fuel composition is a likely reason. This is further discussed below.

It should be noted that the TEC temperature predictions presented in this work do not agree with those presented by Wiinikka et al. [10] for their data. The reason for this is not clear, but one possibility is estimation of BL heat of formation.

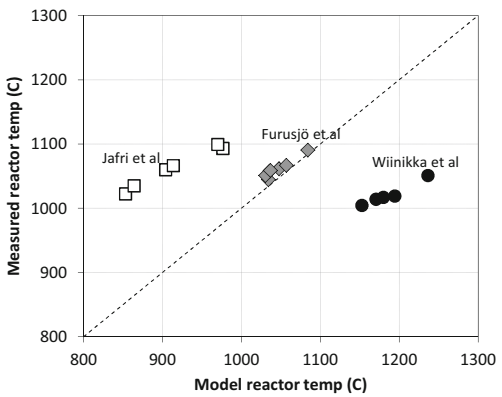

Fig. 3 The relation between measured reactor temperatures and model predictions for the three data sets: Jafri et al. [6] (*black circles*), Wiinikka et al. [10] (*open squares*), Furusjö et al. [12] (*gray diamonds*)

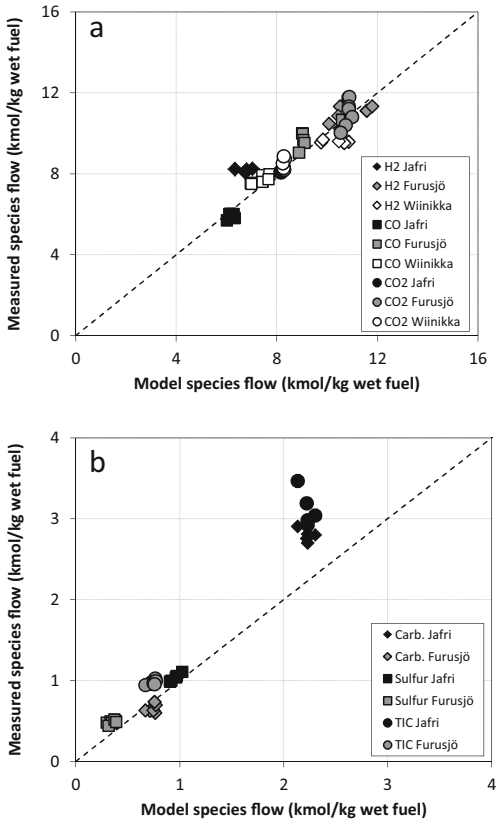

Fig. 4 The relation between measured molar flows for major species and model predictions. Plot (**a**) shows major syngas species. Plot (**b**) shows inorganic species: carbonate, sulfur, and total inorganic carbon (TIC). The three data sets are represented by coloring. No inorganic flow data available for Wiinikka et al. [10]

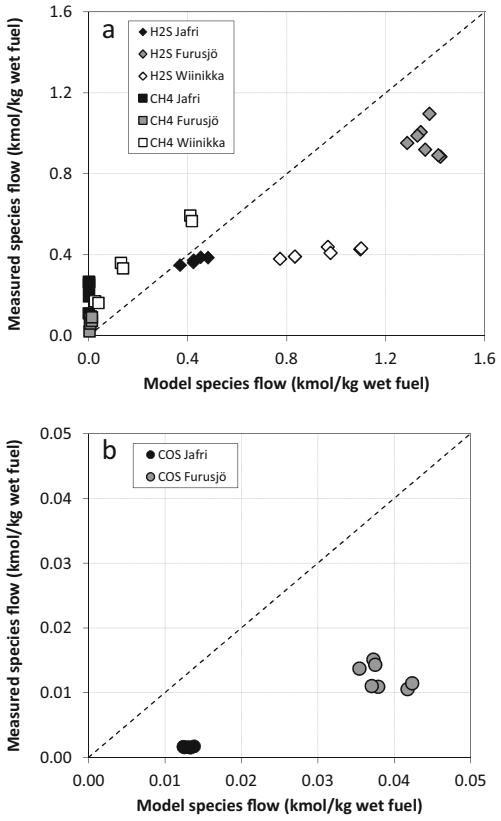

Fig. 5 The relation between measured molar flows for minor syngas species and model predictions. Plot (**a**): H_2S and CH_4. Plot (**b**): COS. The three data sets are represented by coloring. No COS flow data available for Wiinikka et al. [10]

Wiinikka et al. [10] do not specify what assumptions they use regarding combustion products. As discussed in Section 3.1, this can have a very large influence on the calculations.

The predicted flows of major syngas species are fairly consistent with experimental data as shown in Fig. 4, despite the large deviations between model and experimental temperatures. The largest differences are observed for hydrogen but once again with different sign for the two BL data sets (black and white diamonds in Fig. 4a). Data for minor syngas species are shown in Fig. 5. As expected, methane concentrations do not agree well. In fact, TEC methane flows are very close to zero for the Furusjö and Jafri data sets while experimental data shows 0.2–1.5 % of total fuel carbon as methane. For the Wiinikka data set, the model methane flows are more in agreement with experimental data (white squares in Fig. 5a), but this is explained by the very low predicted temperatures for this data set (black squares in Fig. 3) that are not consistent with experimental temperatures. Hence, in agreement with previous studies [7, 10], it can be concluded that methane does not follow thermodynamic equilibrium.

From Fig. 4b, it can be seen that experimental GL TIC is higher than predicted by TECs. This, in combination with the fact that hydrogen carbonate is found in GL but not in the smelt leaving the gasifier, points to the fact that GL absorbs carbon dioxide from the gas, which leads to formation of hydrogen carbonate as shown in Eq. 1. The absorbed amount is, however, not large enough to have any large effect on the carbon dioxide syngas flows as shown in Fig. 4a.

$$Na_2CO_3(aq) + CO_2(g) + H_2O \leftrightarrow 2NaHCO_3(aq) \quad (1)$$

Predictions of GL sulfur are fairly consistent with experimental data as shown in Fig. 4b. It is nevertheless clear from Fig. 5 that H_2S and COS flows are over-predicted. The only exception is H_2S for Jafri et al. (black diamonds in Fig. 5a), which is predicted well, but this (accidental) agreement is an effect of the erroneously high predicted temperature as shown below. For the Furusjö et al. data set, the explanation for the fact that GL sulfur is well predicted but not gas phase sulfur is that the experimental sulfur balances do not close well [12]. Hence, the sulfur split is uncertain for that data set. There is no GL data reported for the data set of Wiinikka et al., so no comparison to experimental GL sulfur is possible. COS experimental flows (Fig. 5b) are much lower than TEC predictions. The likely reason for the lower measured values is not only that equilibrium is not reached in the gasifier but also that COS is known to be hydrolyzed in the quench [9]. Hence, the

COS flow measured in the cool syngas is not representative of the gas leaving the gasifier.

3.3.2 Constraining methane

It has been reported that constraining methane concentration, i.e., accounting for this deviation from equilibrium, in CFD and thermodynamic modeling of BLG has a large effect on predictions of temperatures and major syngas species, especially hydrogen [7]. Constraining the model methane production to the experimental values changes the predicted temperature by 15 ± 4 °C for the BL cases (Jafri et al., Wiinikka et al.) and 4 ± 1.6 °C for the STL case (Furusjö et al.). Considering the differences between model and experimental data in Fig. 3, this difference is not significant. This is partly explained by the fact that methane only accounts for 0.6–1.5 %, 0.8–3.2 %, and 0.2–0.4 % of the total carbon in the feedstock in the data of Jafri et al., Wiinikka et al., and Furusjö et al., respectively.

The major effect of constraining the model methane production, aside from the methane flows themselves, is on hydrogen production in agreement with previous work [7], which decreases by 11 ± 3 % for the BL data sets (Jafri et al., Wiinikka et al.) but only by 1.6 ± 0.6 % for the STL case (Furusjö et al.). Hence, constraining methane improves the agreement between model and experimental values for hydrogen for the Wiinikka et al. data but does the opposite for the Jafri data. Overall, the agreement between model and experimental values for major syngas components is not improved significantly compared to Fig. 4a. The other major deviation from equilibrium, related to sulfur distribution, also has a smaller influence on predictions of other parameters. Clearly, there are other reasons for the deviations between model and experimental data in Figs. 3 and 4.

It should be noted that an adjustment of the Gibbs free energy for methane or the introduction of an activity coefficient can potentially be good alternatives if the aim is to develop a model that can predict methane formation. Such a modification would preferably be based on fitting experimentally observed methane formation for well-validated experimental data. However, initial tests with the data sets used in this work indicate that it is not possible to find a single modification that enables reasonable methane prediction for more than a single data set simultaneously. Similarly, other non-equilibrium species, such as the sulfur species discussed above, can potentially be predicted based on modifications of the thermodynamic equilibrium model.

3.3.3 BL composition adjustment

A systematic deviation of 5–6 % in the experimental carbon balance is present for all OPs in the results of Jafri et al. [6]. No such systematic deviation is present for the other elements investigated (Na, K, S). Hence, flow measurement errors are not likely the reason. The 5–6 % balance error is about twice as large as expected based on reported BL analysis uncertainty and 95 % confidence, cf. Table 2, but fuel analysis error is still a likely main contributor to the observed balance deviation. To test this hypothesis, we adjusted the fuel carbon content for the Jafri et al. data set from that in Table 2 to a higher value that allows the carbon balance to close using experimental data.

Figures 6 and 7 shows the results for the Jafri data set after this adjustment together with the last three OPs of Furusjö et al., which all showed carbon balance closures within 2 % [12]. The data of Wiinikka et al. does not allow balances to be calculated since they did not quantify the inorganic phase and are not included for this reason. The data in Figs. 6 and 7 allows comparison between simulation results and experimental data that does not suffer from large measurement errors (as shown through the good overall and carbon balance closures for these OPs). Hence, the risk of influence from deviations caused by poor experimental data is lower, which means that the real deviation of the process from equilibrium can be studied. From the temperatures shown in Fig. 6, it is clear that the agreement between measured and model temperatures is now excellent for both data sets. The influence of this fuel composition change is dramatic (in comparison with Fig. 3), which is in agreement with the sensitivity to fuel composition observed in Section 3.1 and points out the risk of totally misleading conclusions due to uncertain fuel analysis data.

Figure 7a shows that the BL carbon composition adjustment also gives an improved prediction for major gas components; as an example, the average relative prediction error for hydrogen is reduced from 18 to 5 % despite the fact that no constraint is used for methane. However, the adjustment of fuel composition for the Jafri et al. data does not improve the prediction of minor gas components (not shown) compared to the unadjusted data (Fig. 5). In fact, the hydrogen sulfide flow predictions deviates more after fuel composition adjustment due to the change in model temperature. The

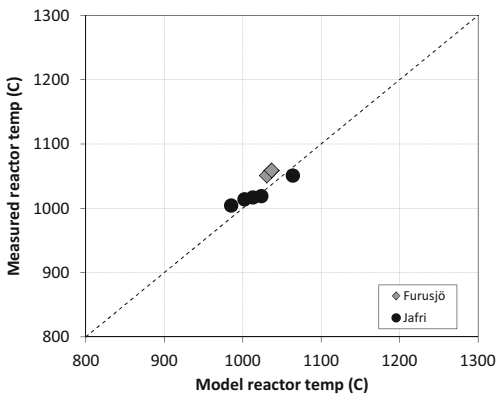

Fig. 6 The relation between measured reactor temperatures and model predictions for selected/adjusted data with good carbon balance closure (see text). Data sets represented by coloring

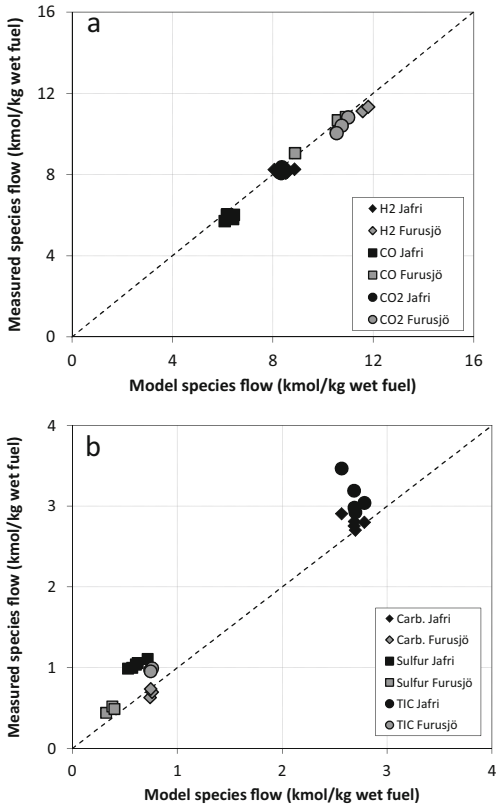

Fig. 7 The relation between measured molar flows for major species and model predictions for selected/adjusted data with good carbon balance closure (see text). Data sets represented by coloring. Plot (**a**) shows major syngas species. Plot (**b**) shows inorganic species: carbonate, sulfur, and total inorganic carbon (TIC)

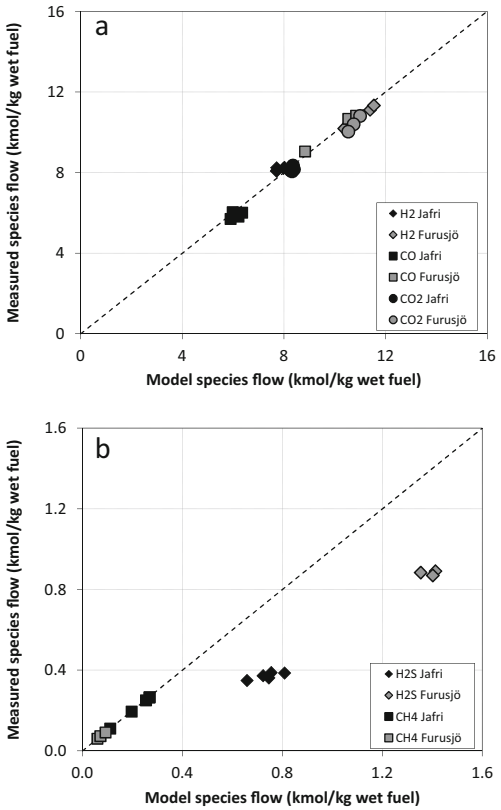

Fig. 8 The relation between measured molar flows for major (**a**) and minor (**b**) syngas species and model predictions. Plot (**a**) shows major syngas species. Plot (**b**) shows H_2S and CH_4. Modeling with constrained CH_4 concentrations using selected data with good carbon balance closure (see text). Data sets represented by coloring

deviation for GL inorganic carbon species does not change and still indicates carbon dioxide absorption in the GL. These results indicate clearly that the deviation in sulfur species and methane are real process deviations from equilibrium.

The much improved agreement between model and experimental data for the Jafri et al. data set after adjusting the fuel C content to match the experimental carbon balance does not prove that fuel analysis error is the sole source of error. It is, however, a strong indication that fuel analysis is a main contributor and once again emphasizes the large influence of fuel analysis on the TEC.

In order to investigate the influence of the non-equilibrium methane behavior on the rest of the components, the same selected data set was used for TECs with methane flows constrained to equal experimental data. The predicted temperature does not change greatly (not shown) and the agreement between model and experimental data for syngas components is improved marginally as shown in Fig. 8. The overall consistency between model and experimental data indicates that TECs can be used to both understand and predict the behavior of EF gasification of spent pulping liquors. The difference between model predictions and experimental data for the major syngas species, as shown in Fig. 8a, is 3 % relative on average with a maximum individual value of 7 %. However, the sulfur gas-smelt distribution still deviates substantially from equilibrium, cf. Fig. 8b.

3.4 Influence of process conditions on process performance

This section investigates the effect on gasifier performance of selected parameters important in the design of a commercial BL or STL gasification-based biorefinery: reactor heat loss, feedstock pre-heat temperature, feedstock DS content, and process pressure. Base case values used are 0.7 % heat loss, 150 °C feedstock pre-heat, 75 % DS, and 30 bar, which are similar to the data from the pilot-scale experiments discussed in Section 3.3 with the exception of heat loss, as discussed below.

Theoretically, the optimum point for operating a gasifier is when exactly enough oxidant is added to avoid formation of elemental carbon and achieve complete gasification [29]. For the gasification process treated in this work, a practical lower temperature limit is around 1000 °C, mainly determined by the fact that very high carbon conversion is required to ensure that pulping chemicals can be recovered [6, 8]. It has been

shown that an optimal temperature with respect to CGE is in the range in which the pilot-scale gasifier is normally operated [10]. Based on data from the previous section, a temperature of 1050 °C is assumed and the required amount of oxygen to reach this temperature is calculated through the gasifier energy balance for the various cases simulated. Thus, the cases with lower heat loss and higher DS content will require a lower oxygen addition to give the required temperature. Moreover, gasification at 1050 °C is assumed to give a methane concentration of 1 vol.% in syngas for BL [6] and 0.2 vol.% for STL [12]. Predictions of fraction of sulfur in the gas cannot be interpreted quantitatively due to the deviations discussed above, but it has been shown that changes in the process lead to changes in the same direction as dictated by equilibrium [7, 8], so trends in model predictions are still useful.

For STL cases, the fuel composition in Table 2 was used. Due to the disagreement between simulations and experimental results for the BL pilot-scale data from Jafri et al. and Wiinikka et al., those BL compositions were not used in this section. Instead, typical BL compositions according to Table 3 were used. The difference between the two BL compositions in Table 3 is electrostatic precipitator (ESP) recycling. Due to fly ash formation in a black liquor RB, a recirculation of ESP ash, up to 10 % of the BL DS flow [30], is normally practiced in Kraft pulp mills. This gives the BL fed to the RB a higher ash content than would otherwise be the case. Since there is no fly ash formation in the gasification process, the rightmost column in Table 3 is relevant for a case where the RB is replaced by a gasifier while the left column can be relevant for a case in which there is an RB and a gasifier in parallel operation. Potassium and chlorine enrichment in ESP ash was disregarded since they are not important for the gasification process. From a gasification point of view, the main effect of removing the ash recycle is that the heating value of the BL increases due to a lower inorganic fraction.

Table 3 BL composition and properties for the study of commercial process performance

		Typical BL, including ash recycle	Typical BL, ESP ash corrected
Dry solids (a.r.)	m/m	75 %	75 %
C (dry)	m/m	33.86 %	36.12 %
H (dry)	m/m	3.45 %	3.71 %
O (dry)	m/m	36.21 %	35.54 %
S (dry)	m/m	5.03 %	4.28 %
Na (dry)	m/m	18.97 %	17.68 %
K (dry)	m/m	2.29 %	2.46 %
N (dry)	m/m	0.08 %	0.09 %
Cl (dry)	m/m	0.11 %	0.12 %
HHV	MJ/kg dry	13.37	14.38
LHV	MJ/kg a.r.	8.85	9.56
SF-LHV[a]	MJ/kg a.r.	7.66	8.55

Figure 9 shows results from TECs with varying heat loss in the interval 0–5 %, where 4.2 % represents the pilot plant cases and 0.5–1 % is a realistic interval for a commercial plant. The influence on CGE is 2–5 % units for different CGEs and different feedstocks. This shows that energy efficiency will be better in commercial scale. The influence on H_2/CO and sulfur split is very limited (not shown), which indicates that pilot-scale experiments can be relevant for predicting at least H_2/CO. For the sulfur split, it is not known if the deviation from equilibrium, which is substantial, is dependent on scale. Successive simulations, discussed below, were done at 0.7 % heat loss, which is considered relevant for a commercial-scale plant.

Varying feedstock pre-heat (not shown) is analogous to changing the reactor heat loss from a TEC point of view; heat loss is a negative term in the gasifier energy balance while feedstock sensible heat is a positive term. The 100 °C temperature interval investigated for feedstock pre-heat corresponds to a 1.9–2.7 % difference in sensible energy compared to the feedstock heating value (HHV), which is about half of the interval studied for heat loss. Consequently, the effect on CGE is about half of that in Fig. 9.

The CGE for HHV in Fig. 9 (lines without symbols) show that practically 100 % of any heat that is added through either increased pre-heating or decreased heat loss is converted to chemical energy in the gas. This is a consequence of the energy balance of the gasifier since the smelt chemical and sensible energy is largely unaffected by the change due to the constant temperature used in these simulations. As noted above, less oxygen is required to reach 1050 °C if heat losses are lower. Decreasing heat loss or increasing pre-heating can thus be viewed as converting thermal energy to chemical energy with 100 % efficiency. It should be noted that varying feedstock pre-heat can also have other effects on the

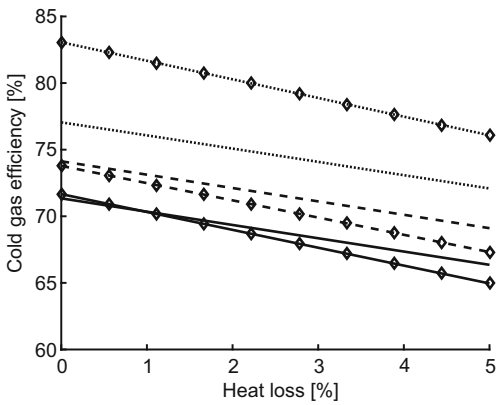

Fig. 9 Influence of reactor heat loss on cold gas efficiency on HHV basis (*lines*) and H_2 + CO S-free LHV basis (*diamonds*) for the three feedstock compositions BL (*solid*), ash recycle adjusted BL (*dashed*), and STL (*dotted*)

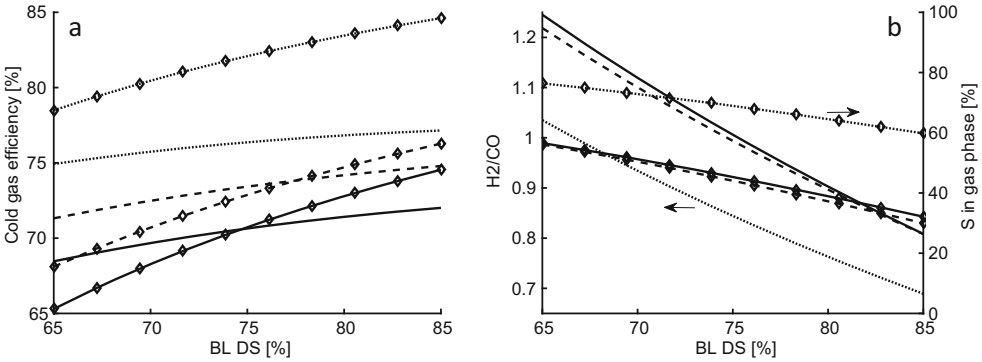

Fig. 10 Influence of feedstock DS content for typical BL (*solid*), ash recycle adjusted BL (*dashed*), and STL (*dotted*). Plot (**a**): cold gas efficiency on HHV basis (*lines*) and H_2 + CO S-free LHV basis (*diamonds*). Plot (**b**): H_2/CO (*lines*, *left axis*) and S in gas phase (*diamonds*, *right axis*)

gasification, e.g., gas phase sulfur and methane formation [8], but these effects cannot be predicted by TECs.

An industrially relevant interval for BL DS content is 65–85 %, with 65 % representing old pulp mills or mills with liquors that are particularly difficult to concentrate and 85 % representing a future scenario. Modern mills typically reach 80 % DS [30]. It is evident from Fig. 10 that feedstock DS content has a strong influence on the process, which is not surprising given that a 65 % DS liquor contains three times more water per kilogram of solids than an 85 % liquor. Due to the high process temperature, the penalty for added thermal ballast is significant.

The only major effect of pressure in the interval 5–60 bar is on the sulfur distribution. For BL, the sulfur split increases from 20 to 60 % when increasing the pressure from 5 to 60 bar, as shown in Fig. 11. The influence on HHV CGE seen in Fig. 11a is simply an effect of this sulfur shift since syngas HHV includes contribution from S species, as evidenced by the lack of effect on CGE on S-free LHV basis. Wiinikka et al. [10] showed that equilibrium methane concentrations increase with pressure. Our results show the same behavior, but the effect is relatively small and, as discussed above, thermodynamic equilibrium methane predictions are far from experimental values.

In general, the results in Figs. 9, 10, and 11 clearly show the effect of inorganic ballast; the STL feedstock with approximately half the inorganic content of BL has a significantly higher CGE in all cases. There is also a substantial effect from the recycled ash, as shown by the different CGE values for the typical BL and the ash recycle adjusted BL, which has approximately 10 % lower sodium content. In addition, the fraction of sulfur that ends up in the gas phase is much higher for the STL case. This is explained by the proportions between sulfur and sodium/potassium in the different feedstocks. For STL, the molar S/$(Na + K)_2$ ratio is 1.6 which means that even if all sodium formed sodium sulfide, 40 % of the sulfur would go into the gas phase. In practice, more sulfur ends up in syngas due to the equilibrium between sodium sulfide and sodium carbonate.

Oxygen is a significant cost for operating a gasifier of this type [5]. Simulation results show a large effect on oxygen consumption from some of the parameters studied, e.g., a reduction of 33 % when increasing DS from 65 to 85 % for the ash-corrected BL. Generally, any change that improves CGE also decreases specific oxygen consumption. This is simply a consequence of the fact that added oxygen is used to oxidize feedstock to obtain the required heat for the process.

4 Conclusions

The high temperature and the catalytic activity of feedstock alkali makes thermodynamic equilibrium a better predictor of product composition in EFG of spent pulping liquors than for

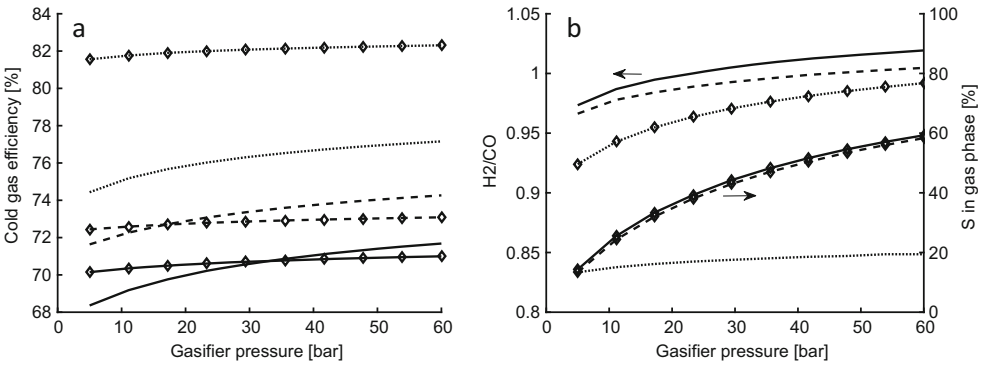

Fig. 11 Influence of process pressure for typical BL (*solid*), ash recycle adjusted BL (*dashed*), and STL (*dotted*). Plot (**a**): cold gas efficiency on HHV basis (*lines*) and H_2 + CO S-free LHV basis (*diamonds*). Plot (**b**): H_2/CO (*lines*, *left axis*) and S in gas phase (*diamonds*, *right axis*)

many other types of biomass and gasification technologies. TECs can predict the flows of the main syngas and slag products with high accuracy as shown by comparison with experimental data with small measurement errors.

Small changes in feedstock composition have a relatively large influence on the thermodynamic equilibrium model predictions. This means that the model is sensitive to any errors in input data due to analytical uncertainty. However, since it was also concluded that the process follows thermodynamic equilibrium fairly well, this also means that the process itself is sensitive to naturally occurring variations in feedstock composition, e.g., due to seasonal changes, which can influence important operating parameters such as oxygen consumption and CGE. This is important knowledge for further research and process design.

The main process deviations from equilibrium are methane formation and sulfur distribution between gas and slag. Constraining methane to the experimental value improves prediction accuracy of other gas species. Investigating the possibility of implementing empirical modifications to the equilibrium model in order to predict methane and sulfur split are important areas for further research. The full carbon conversion predicted by the thermodynamic equilibrium model is not a major deviation from the real process, which is in contrast to modeling other biomass gasification technologies.

The gasification of BL and STL gives a different product distribution, due to the different feedstock compositions, but can be described with the same thermodynamic equilibrium model with the same main deviations from experimental data. This indicates that gasification of other fuels with similar properties, e.g., high alkali content, may also be possible to describe using the same model.

The simulations of a commercial-scale gasification process show that CGE on S-free LHV basis can reach over 80 %. There are large efficiency gains connected to reducing ballast, in the form of water or inorganics, as well as reducing heat losses. The on-going work with BL/pyrolysis oil blends is one possible way to decrease inorganic ballast while maintaining the high reactivity and carbon conversion.

Acknowledgements The Swedish Energy Agency and an industrial consortium are acknowledged for financial support to the LTU Biosyngas Program in which the research described in this article was undertaken. Henrik Wiinikka and Jonas Wennebro at SP-ETC (Piteå, Sweden) are acknowledged for discussions around heat of formation for high ash fuels.

References

1. Landälv I, Gebart R, Marke B et al (2014) Two years experience of the BioDME project—a complete wood to wheel concept. Environ Prog Sustain Energy 33:744–750
2. Larson ED, Consonni S, Katofsky RE et al (2009) An assessment of gasification-based biorefining at kraft pulp and paper mills in the United States, part B: results. TAPPI J 8:27–35
3. Consonni S, Katofsky RE, Larson ED (2009) A gasification-based biorefinery for the pulp and paper industry. Chem Eng Res Des 87:1293–1317. doi:10.1016/j.cherd.2009.07.017
4. Pettersson K, Harvey S (2012) Comparison of black liquor gasification with other pulping biorefinery concepts—systems analysis of economic performance and CO_2 emissions. Energy 37:136–153. doi:10.1016/j.energy.2011.10.020
5. Andersson J, Furusjö E, Wetterlund E et al (2016) Co-gasification of black liquor and pyrolysis oil: evaluation of blend ratios and methanol production capacities. Energy Convers Manag 110:240–248. doi:10.1016/j.enconman.2015.12.027
6. Jafri Y, Furusjö E, Kirtania K, Gebart R (2016) Performance of an entrained-flow black liquor gasifier. Energy Fuel 30:3175–3185. doi:10.1021/acs.energyfuels.6b00349
7. Carlsson P, Marklund M, Furusjö E et al (2010) Experiments and mathematical models of black liquor gasification—influence of minor gas components on temperature, gas composition, and fixed carbon conversion. TAPPI J 9:15–24
8. Carlsson P, Wiinikka H, Marklund M et al (2010) Experimental investigation of an industrial scale black liquor gasifier. 1. The effect of reactor operation parameters on product gas composition. Fuel 89:4025–4034. doi:10.1016/j.fuel.2010.05.003
9. Wiinikka H, Carlsson P, Marklund M et al (2012) Experimental investigation of an industrial scale black liquor gasifier. Part 2: influence of quench operation on product gas composition. Fuel 93:117–129. doi:10.1016/j.fuel.2011.06.066
10. Wiinikka H, Johansson A-C, Wennebro J et al (2015) Evaluation of black liquor gasification intended for synthetic fuel or power production. Fuel Process Technol 139:216–225. doi:10.1016/j.fuproc.2015.06.050
11. Furusjö E, Stare R, Häggström, S (2010) Gasification of thick liquor from a sulfite cellulose mill using pressurized high temperature entrained flow gasification. In: Int. Chem. Recover. Conf. Williamsburg, VA, 29 March–1 April 2010. TAPPI, Atlanta, GA, pp 270–78
12. Furusjö E, Stare R, Landälv I, Löwnertz P (2014) Pilot scale gasification of spent cooking liquor from sodium sulfite based delignification. Energy Fuel 28:7517–7526. doi:10.1021/ef501753h
13. Ptasinski KJ (2008) Thermodynamic efficiency of biomass gasification and biofuels conversion. Biofuels, Bioprod Biorefining 2:239–253. doi:10.1002/bbb.65
14. Puig-Arnavat M, Bruno JC, Coronas A (2010) Review and analysis of biomass gasification models. Renew Sust Energ Rev 14:2841–2851. doi:10.1016/j.rser.2010.07.030
15. Baruah D, Baruah DC (2014) Modeling of biomass gasification: a review. Renew Sust Energ Rev 39:806–815. doi:10.1016/j.rser.2014.07.129
16. Zainal ZA, Ali R, Lean CH, Seetharamu KN (2001) Prediction of performance of a downdraft gasifier using equilibrium modeling for different biomass materials. Energy Convers Manag 42:1499–1515. doi:10.1016/S0196-8904(00)00078-9
17. Altafini CR, Wander PR, Barreto RM (2003) Prediction of the working parameters of a wood waste gasifier through an equilibrium model. Energy Convers Manag 44:2763–2777. doi:10.1016/S0196-8904(03)00025-6

18. Jarungthammachote S, Dutta A (2008) Equilibrium modeling of gasification: Gibbs free energy minimization approach and its application to spouted bed and spout-fluid bed gasifiers. Energy Convers Manag 49:1345–1356. doi:10.1016/j.enconman.2008.01.006
19. Rofouie P, Moshkelani M, Perrier M, Paris J (2014) A modified thermodynamic equilibrium model for woody biomass gasification. Can J Chem Eng 92:593–602. doi:10.1002/cjce.21926
20. Huang HJ, Ramaswamy S (2009) Modeling biomass gasification using thermodynamic equilibrium approach. Appl Biochem Biotechnol 154:193–204. doi:10.1007/s12010-008-8483-x
21. Carlsson P, Ma C, Molinder R et al (2014) Slag formation during oxygen-blown entrained-flow gasification of stem wood. Energy and Fuels 28:6941–6952. doi:10.1021/ef501496q
22. Ma C, Backman R, Öhman M (2015) Thermochemical equilibrium study of slag formation during pressurized entrained-flow gasification of woody biomass. Energy and Fuels 29:4399–4406. doi:10.1021/acs.energyfuels.5b00889
23. Berglin N (1996) Pulp mill energy systems with black liquor gasification—a process integration study. Dissertation, Chalmers University of Technology
24. Backman R, Salmenoja K (1994) Equilibrium behaviour of sodium, sulfur and chlorine in pressurized black liquor gasification with addition of titanium oxide. Pap ja puu 76:320–325
25. Backman R, Frederick WJ, Hupa M (1993) Basic studies on black-liquor pyrolysis and char gasification. Bioresour Technol 46:153–158. doi:10.1016/0960-8524(93)90067-L
26. Huang H, Ramaswamy S (2011) Thermodynamic analysis of black liquor steam gasification. Bioresources 6:3210–3230. doi:10.15376/biores.6.3.3210-3230
27. Andersson J, Lundgren J, Furusjö E, Landälv I (2015) Co-gasification of pyrolysis oil and black liquor for methanol production. Fuel 158:451–459. doi:10.1016/j.fuel.2015.05.044
28. Lindberg D (2007) Thermochemistry and melting properties of alkali salt mixtures in black liquor conversion processes. Dissertation, Åbo Akademi University
29. Prins MJ, Ptasinski KJ, Janssen FJJG (2003) Thermodynamics of gas-char reactions: first and second law analysis. Chem Eng Sci 58:1003–1011. doi:10.1016/S0009-2509(02)00641-3
30. Vakkilainen EK (2005) Kraft recovery boilers: principles and practice, 2nd edn. Suomen Soodakattilayhdistys r.y, Helsinki